Geophysical Research Letters

RESEARCH LETTER
10.1029/2023GL106082

Filtering of the Signal of Sediment Export From a Glacier by Its Proglacial Forefield

D. Mancini[1], M. Dietze[2,3], T. Müller[1], M. Jenkin[1], F. Miesen[1], M. Roncoroni[1], A. P. Nicholas[4], and S. N. Lane[1]

[1]Institute of Earth Surface Dynamics (IDYST), Université de Lausanne, Lausanne, Switzerland, [2]Institute of Geography, Georg-August-University Göttingen, Göttingen, Germany, [3]German Research Center for Geosciences (GFZ), Potsdam, Germany, [4]Geography, Faculty of Environment, Science and Economy, University of Exeter, Exeter, UK

Key Points:

- Seismically inferred sediment transport anatomy reveals strong filtering of subglacial bedload export signal due to proglacial processes
- Filtering operates at a sub-daily scale, and is due to the short advection lengths of bedload particles in the proglacial forefield
- Proglacial filtering is a key factor affecting (pro-)glacial sediment transport dynamics, sediment connectivity and ecological succession

Supporting Information:

Supporting Information may be found in the online version of this article.

Correspondence to:

D. Mancini,
davide.mancini@unil.ch

Citation:

Mancini, D., Dietze, M., Müller, T., Jenkin, M., Miesen, F., Roncoroni, M., et al. (2023). Filtering of the signal of sediment export from a glacier by its proglacial forefield. *Geophysical Research Letters*, *50*, e2023GL106082. https://doi.org/10.1029/2023GL106082

Received 25 AUG 2023
Accepted 3 OCT 2023

Author Contributions:

Conceptualization: D. Mancini, A. P. Nicholas, S. N. Lane
Data curation: D. Mancini, T. Müller, M. Jenkin, F. Miesen, M. Roncoroni, S. N. Lane
Formal analysis: D. Mancini, M. Dietze, S. N. Lane
Funding acquisition: A. P. Nicholas, S. N. Lane
Investigation: D. Mancini, S. N. Lane
Methodology: D. Mancini, M. Dietze, S. N. Lane

Abstract Alpine glaciers are rapidly retreating due to global warming and this has been associated with enhanced supply of subglacially derived sediment to downstream environments. We present the first high frequency quantitative record on how the signal of sediment exported from an Alpine glacier is filtered by its proglacial forefield. The data, covering two climatically distinct glacier melt seasons, show that the signal of subglacial bedload export is strongly filtered over short distances, unlike suspended load whose signal is less impacted. The reason is related to the interplay of short particle advection lengths with strong morphodynamic forcing. The subglacial sediment export signal is thus rapidly replaced by one combining (a) the local forcing by stream hydraulics and (b) the reworking of the proglacial braid plain itself. These findings have implications for estimating subglacial erosion rates, natural hazard mitigation, sediment management for hydropower plants and ecological succession related to rapid glacier retreat.

Plain Language Summary Alpine glaciers have been retreating at increasing rates since the early 20th century due to the current climate warming. As a consequence, new, powerful and rapidly changing rivers have developed in the newly emerged terrain in front of shrinking glaciers (i.e., proglacial forefields). These environments are known to be among the most rapidly changing landscapes on Earth. In this study we present the first combined high frequency quantitative data on sediment export from an Alpine glacier for two melt seasons with very different climatic conditions. Results show that the low potential transport distances of particles traveling on the river bed together with the continuously changing shape of these streams, rapidly modify the glacier-dictated export signal (i.e., subglacial sediment evacuation rates in time). For sediment transported in suspension in the river, that loss of information is less evident. These findings are important for the understanding of how much, when, and which kind of sediment are delivered to the populated places downstream in the valleys, in order to mitigate natural hazards, but also for sediment management in hydropower plants and ecological succession in the context of rapid glacier retreat. The results are also key to improving estimation of glacial erosion rates.

1. Introduction

Mountain glaciers and ice sheets are retreating globally (Moon, 2017). In the European Alps glaciers lost about 50% of their surface between 1850 and 2000 (Zemp et al., 2006). This rapid retreat results in rapidly growing proglacial margins which, in the Swiss and Austrian Alps alone, consist of ca. 930 km^2 of deglaciated terrain exposed since the end of the Little Ice Age (Carrivick et al., 2018). Concurrently, increasing subglacial sediment evacuation rates (Lane et al., 2017) impact the morphodynamics of the forefields that form downstream of glaciers given the observed influence of sediment supply (Ashmore, 1988, 1991a; Lane et al., 1996).

Sediment flux in geomorphic systems including alluvial rivers (e.g., Ashmore, 1991a), hillslope- catchment systems (e.g., Hasbargen & Paola, 2000; Lancaster & Casebeer, 2007) and river deltas (e.g., Kim et al., 2006; van Dijk et al., 2009) is characterized by significant temporal variability (Coulthard et al., 2005; Phillips, 2003). Variability is not only a function of external forcing, such as precipitation events or daily discharge variations, but is also induced by autogenic processes resulting in self-organizing behavior (Carling et al., 2016; Coulthard & Van De Wiel, 2007) and the strong filtering of exogenic forcing over a wide range of timescales (Jerolmack & Paola, 2010). Such filtering has been attributed to two related scales of behavior: (a) progressive reworking of fluvial landforms (Beerbower, 1964), meaning that sediment cannot always pass easily through a river reach

Project Administration: A. P. Nicholas, S. N. Lane
Resources: S. N. Lane
Software: D. Mancini, M. Dietze
Supervision: A. P. Nicholas, S. N. Lane
Writing – original draft: D. Mancini
Writing – review & editing: D. Mancini, M. Dietze, T. Müller, M. Jenkin, F. Miesen, M. Roncoroni, A. P. Nicholas, S. N. Lane

without encountering a depositional environment; and (b) limits on the advection length for sediment, which are a function of ambient flow velocity, particle settling height and particle size (Ganti et al., 2014). The former are well known for proglacial margins (e.g., bank failure following lateral erosion, in-channel and alluvial channel storage, channel bifurcation, avulsion and channel abandonment,…) (Ashmore, 1991b; Cudden & Hoey, 2003; Hundey & Ashmore, 2009; Kasprak et al., 2015; Van De Wiel & Coulthard, 2010). Advection limits are related to this morphological forcing. For instance, Kasprak et al. (2015) found that the particle displacement lengths in a laboratory flume vary with the mean distance between confluences and diffluences. This is because diffluences set maximum advection lengths by promoting flow deceleration and a local reduction in settling height (Ashworth, 1996) and so deposition.

The above statements suggest that proglacial forefields have the potential to filter the signal of sediment exported from glaciers, but the extent to which this might be the case has never been demonstrated. Our current knowledge of subglacial sediment export by glacier-fed streams is dominated by suspended sediment monitoring (e.g., Delaney et al., 2018; Richards, 1984; Swift et al., 2005), only one part of the sediment export signal. Difficulties in measuring bedload transport have resulted in major uncertainties in absolute bedload amounts, the relative importance and temporal variation of bedload and suspended load transport rates in both glacial and proglacial environments, and how rates vary from the event scale to the diurnal, seasonal and eventually multi-year scales. As yet, we have no continuous records of bedload transport in proglacial marginal settings.

Morphodynamic filtering of downstream sediment transport signals can occur to different degrees, including (a) dampening when the signal amplitude is scaled down but the amplitude-frequency dependence remains; (b) delaying which may or may not accompany dampening but where there is a shift in phase; and (c) shredding where the amplitude-frequency dependence is partially or completely destroyed (Straub et al., 2020). Understanding the extent to which there is filtering and the distance over which it occurs is important for several disciplines. Glaciologists commonly estimate glacial erosion rates from subglacial sediment export measurements (Herman et al., 2015; Humphrey & Raymond, 1994; Riihimaki et al., 2005; Swift et al., 2005) and relate these to contemporaneous measurements of ice sliding velocity (i.e., sliding erosion law; Amundson & Iverson, 2006). The non-linear relationship between glacier sliding velocity and measured erosion rates remains highly uncertain (Cook et al., 2020) due to difficulties in correctly inferring the erosion rate itself. Sediment transport rates are commonly determined from fixed installations located several kilometers away from glacier termini (e.g., Carrillo & Mao, 2020; Comiti et al., 2019; Delaney et al., 2018; Dell'Agnese et al., 2014), potentially obscuring recorded sediment transport rates in the presence of signal filtering. A dampened signal may translate into errors in the magnitude of estimated transport rates. A delayed signal may cause temporal uncertainty in which ice velocity variation should be related to erosion rate variation. A partially shredded signal may contain only a partial signals of glacial erosion. A completely shredded signal may still provide a reliable long-term mean erosion rate but no signal of variation in glacial erosion.

Here, we present the first high-frequency, continuous, seasonal-scale data for bedload, accompanied by suspended load, for a proglacial margin. The data allow us to quantify how proglacial morphodynamics filter the signal of the sediment exported from the snout margin of an Alpine glacier for both suspended load and bedload in a context of rapid deglaciation, and the timescale over which the filtering occurs. This is achieved by combining passive seismic monitoring and more classical discharge and suspended sediment load measurements.

2. Methods

The study is focused on the Glacier d'Otemma proglacial margin (Figure 1) located in the southern-western Swiss Alps (Bagnes Valley, Valais) at an altitude of about 2,450 m a.s.l.. The proglacial forefield is ca. 1 km long and ca. 200 m wide with a mean valley bottom slope of about 1.2%. The configuration of the proglacial stream follows the available accommodation space, limited by steep valley sidewalls, and the valley bottom slope. Where the lateral accommodation space is at a maximum, and slope is lower (mean of 0.18%), the channel pattern is dominated by an active braided network. Toward the upstream glacier terminus and at the downstream forefield end, flow is confined into a single bedrock-dominated channel due to the combination of a narrower and steeper (3.18%) valley section. The proglacial stream flows on a bed mostly composed of quaternary morainic deposits with a mixed sand, gravel and cobble particle size range: close to the glacier terminus the texture of the riverbed is dominated by gravels and cobbles (D_{50} of ca. 78 mm and D_{84} of ca. 92 mm, $n = 345$), while toward the forefield end more sandy deposits are also present (D_{50} of ca. 37 mm and D_{84} of ca. 48 mm, $n = 348$).

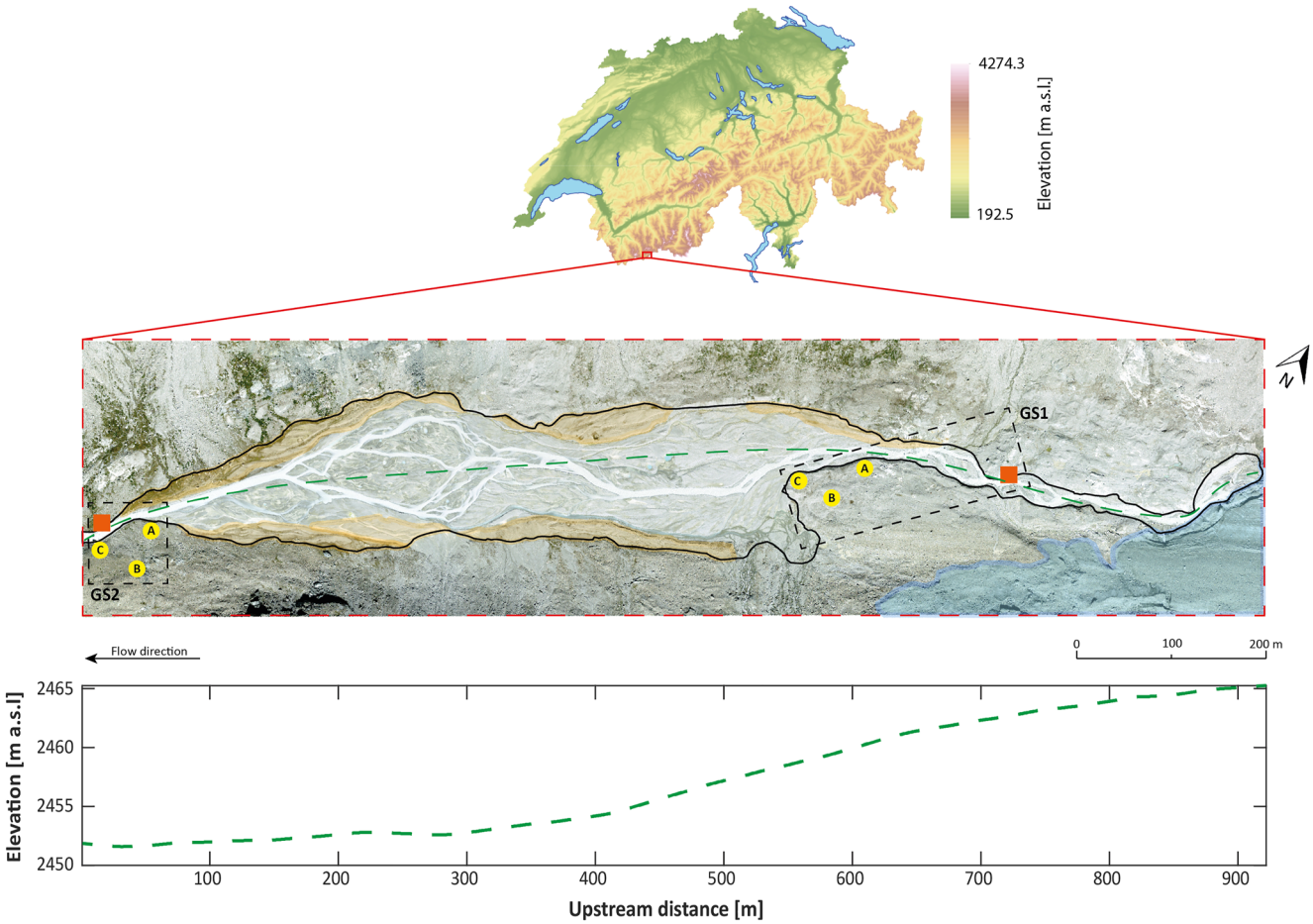

Figure 1. Location of GS1 and GS2 in the Glacier d'Otemma proglacial forefield. Yellow circles refer to geophones, orange squares to turbidity probes and water pressure sensors, the light blue region highlights baer and debris-covered glacier, while orange regions the terraces and the black line the proglacial forefield limits. The green dashed line is the elevation profile.

This proglacial forefield was chosen for two reasons. First, Mancini and Lane (2020) showed that the forefield and the valley sidewalls were largely disconnected from each other due to the development of alluvial fans that buffer hillslope to forefield sediment flux. Second, the active forefield is located within stable terrace systems reflecting a long-term state of sediment supply being lower than potential transport capacity (Collins, 2008; Marren & Toomath, 2013; Roussel et al., 2018). Thus, the glacier is the primary source of both suspended load and bedload. We studied two melt seasons experiencing different climatic conditions (Text S1 in Supporting Information S1): summer 2020 from 25th June (Julian Day [JD] 177) to 29th August (JD 242), which was warmer and drier; and summer 2021 from 11th June (JD 162) to 21st August (JD 233), which was colder and wetter especially in the first part of the season.

Continuous suspended load and bedload transport rates were indirectly monitored at two gauging stations located ca. 350 m from the glacier terminus (GS1) and at the forefield outlet (GS2) with a distance of ca. 850 m between them (Figure 1). They were equipped with turbidity probes, water pressure sensors and geophones. Suspended loads were derived using a conventional turbidity-sediment concentration relationship (Texts S2 and S3 in Supporting Information S1), whilst bedload transport was monitored seismically (Texts S4–S7 in Supporting Information S1). The post-processing of collected seismic data to quantify bedload transport rates used the geophysical inversion model of Dietze et al. (2019) in the open source R package *eseis* (version 0.5.0) (Dietze, 2018; Text S4 in Supporting Information S1). Model calibrations for both GS1 and GS2 are explained in Texts S4 through S7 of the Supporting Information S1. Given the extreme difficulty of direct measurement of bedload (e.g., with a portable sampler) in this kind of river, we used the fact that water stage is an output of the seismic inversion which if successful should reproduce water stages measured at GS1 and GS2 (Texts S5 through

S7 in Supporting Information S1). Second, in 2021, we installed an additional station at the glacier terminus (GSG) 300 m upstream of GS1. With a relatively straight steep, semi-alluvial reach between GS1 and GSG we expected them to have similar signals and so used GSG as a control on the repeatability of the method (Figure 1; Text S6 in Supporting Information S1). Finally, recognizing that the inversion model contains parameters (e.g., ground proprieties) that are unlikely to be stationary, we applied Latin Hypercube Sampling to plausible parameter ranges to estimate uncertainty in each seismically estimated bedload transport rate (Text S4 in Supporting Information S1).

We combined analysis of sediment transport time-series with power spectra to detect the kind and nature of filtering of the signals traveling through the floodplain (Text S8 in Supporting Information S1). We compared correlations of water discharge and sediment transport signals, both suspended sediment load and bedload, at GS1 and GS2 to determine spatial differences in transport dynamics. Results were combined with cross-correlation of signals monitored at GS1 and GS2 to define the nature of the proglacial forefield filtering on them. This latter aspect was then further investigated using power spectra analysis following Jerolmack and Paola (2010) (Text S8 in Supporting Information S1). This approach applies a Discrete Fourier Transform to both instantaneous suspended sediment load and bedload signals at GS1 and GS2 to convert them from the time into the frequency domain. Frequencies were then converted into timescales (days) by relating them to their sampling interval (i.e., 2 min; 0.00014 JD), while amplitudes were squared to convert them from complex number into powers ($10\log_{10}(\mathrm{kg/s})^2$, hence dB). We expected fluctuations in power to increase as a power-law function of time within timescales having significant variability in sediment flux (i.e., sub-daily to daily), followed by a situation marked by only slight increases at longer timescales (i.e., seasonal). If the forefield acts as a non-linear filter, the power-period relations for GS1 and GS2 should have non-zero slopes, with the local gradient of the spectrum proportional to the filtering magnitude. The spatial comparison of spectra allows determining how the forefield has filtered the signal. At the same time, we also assessed if the diurnal suspended sediment load and bedload export signals are still recorded at the forefield outlet by comparing the daily export periodicity to the characteristic timescale of the system.

Once both filter strength and timescales were determined, we investigated the responsible morphodynamic filtering mechanisms (Text S8 in Supporting Information S1). We calculated the difference between GS1 and GS2 in the timing of discharge, suspended load and bedload signal peaks, assuming a straight-line travel distance, to derive a measure of the virtual velocities (V_v) of water and sediment waves following Hassan et al. (1991). It is important to note here that the braided nature of the reach should increase the effective travel distance calculations giving maximum possible velocities. Then, by knowing for each transport cycle the duration for which discharge exceeded the transport capacity threshold Q_c, calculated according to Rickenmann (1991), we were able to retrieve daily advection lengths. The latter were defined as the distance traveled by a particle before it settles to the bed (Ganti et al., 2014). We derived them by multiplying the virtual propagation velocities of the suspended sediment load and the bedload waves by the daily duration for which discharge was higher then Q_c. As shown in Métivier (1999), for a sediment transport signal to be modified between two points in space the length-scales of transporting events (i.e., their advection lengths) must be shorter than the distance between those points, in this case GS1 and GS2 (Figure 1). This is related to the different propagation velocities of discharge and sediment waves, and it reflects the observation of Ganti et al. (2014) that the bounds on advection lengths are constrained by sediment settling velocities. Finally, we used the daily Shannon Entropy index (SE) (Lane & Nienow, 2019) to study the relationship between the changing variability of transport signals at GS1 and GS2 and discharge variation during the melt season (SE index is proportional to signal variability: higher values means a more spread-out distribution). Assuming sediment export from the glacier tracks discharge, we would expect signal filtering to manifest as a reduction in the intensity of daily transport variation and hence a reduction in Shannon Entropy.

3. Suspended Sediment Load and Bedload Transport Dynamics

Daily hydrographs have an asymmetrical shape characterized by: rapid increase during the rising limb, starting around 10 a.m., to maxima of ca. 13.5 m^3/s in 2020 and of ca. 11 m^3/s in 2021; followed by a gentler decrease in the falling limb, usually starting around 6 p.m. (Q_w, Figure 2a). Suspended sediment load reflects this variation at GS1 and GS2 for both melt seasons with discharge versus suspended sediment load (Q_s) correlations of 0.632 (2020, $p < 0.05$) and 0.681 (2021, $p < 0.05$) for GS1 and 0. 574 (2020, $p < 0.05$) and 0.557 (2021, $p < 0.05$) for GS2. As discharge increases, (a) suspended load increases at both sites with only small differences in magnitude

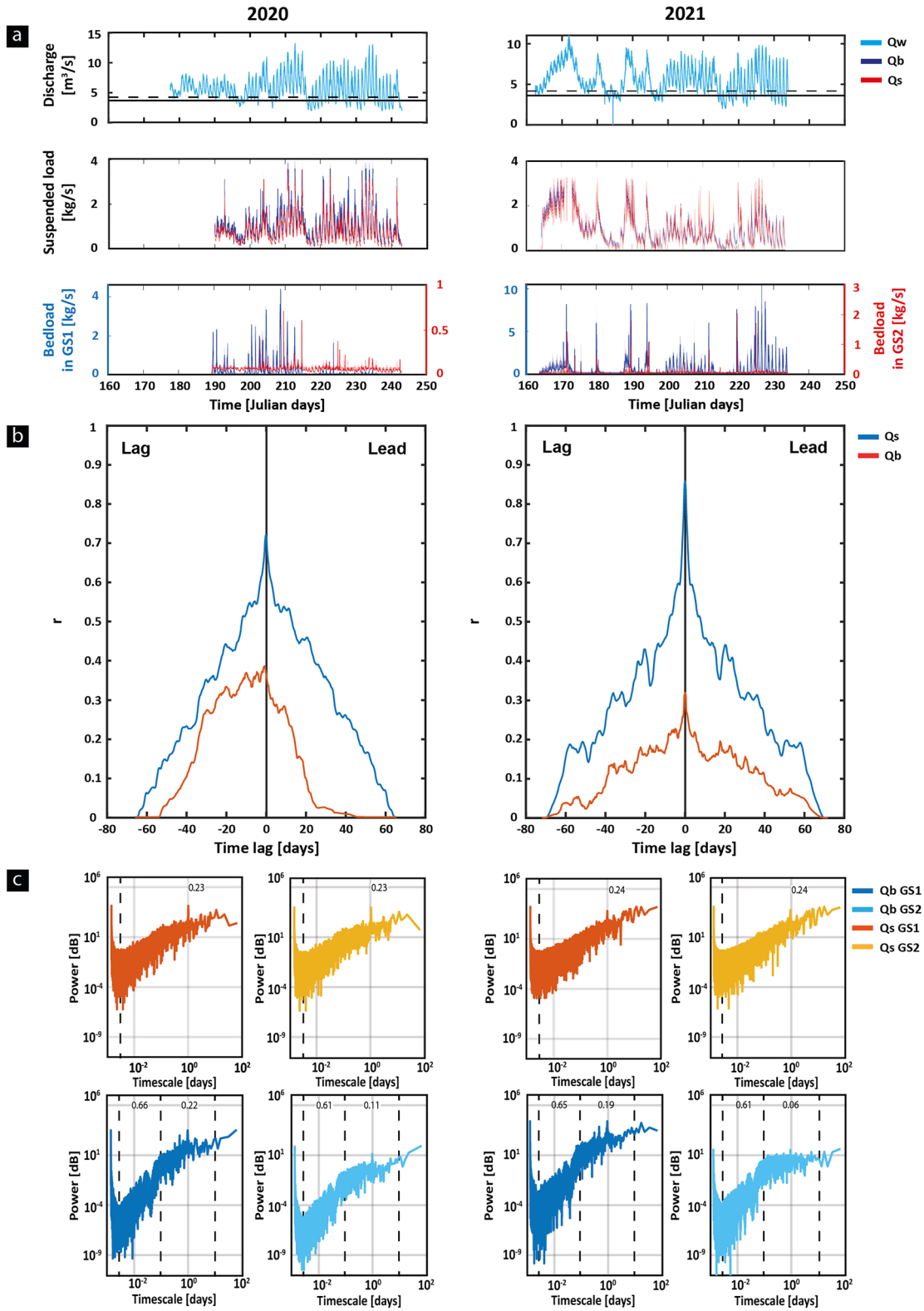

Figure 2. Timeseries and analyses on transport signals revealing the proglacial filtering. Field collected discharge, suspended sediment load and bedload time series (a; dashed and solid black lines refer to Q_c in GS1 and GS2, respectively). Cross-correlation of suspended sediment load and bedload signals at GS1 and GS2: a 1 day running mean is applied to raw correlations to remove diurnal variations and long-term structures. Lag (lead) means that peak at GS1 occurs earlier (later) than at GS2 (b). Power spectra of instantaneous transport rates (c).

between sites; (b) maximum loads coincide with maximum discharges at both sites; but (c), during daily hydrograph recession, loads diverge with GS1 values higher than GS2 values. Given the absence of river-connected kettle holes and lakes that have been shown to buffer proglacial suspended sediment flux (Bogen et al., 2014; Geilhausen et al., 2013), these differences are likely due to local temporary trapping of fine sediment due to bed roughness (Parsons et al., 2018), the incorporation of fine sediment during falling limb bar formation (Orwin & Smart, 2004; Richards, 1984) and overbank fine sediment deposition.

Bedload transport rates (Q_b; Figure 2a) also show some association with discharge but correlations are only significant upstream at GS1 (0.437 and 0.611 for 2020 and 2021 respectively, $p < 0.05$ in both cases) and not downstream at GS2 (0.309 and 0.162 for 2020 and 2021 respectively, $p > 0.05$ in both cases), suggesting the breakdown of capacity-driven bedload transport due to the presence of the proglacial forefield. While there can be a significant suspended load at all discharges, bedload seems to be delayed compared to discharge closer to the glacier at GS1 (Beaud, Flowers, & Venditti, 2018; Beaud, Venditti, et al., 2018; Beaud et al., 2016) and strongly threshold-limited at GS2 (Perolo et al., 2019). In 2021, the correlation between Q_b and Q_w is similar (0.611) to Q_s and Q (0.681) at GS1. However, the Q_b and Q_w correlation at GS1 is lower in 2020 (0.437) than for Q_s (0.632) because subglacial sediment export rates, and hence the transport rates measured at GS1, reduced significantly from early August onwards. The correlation between Q_b and Q_w at GS1 was 0.522 until 5th August when this reduction occurred.

4. Filtering of Subglacial Sediment Export Signals by Forefield Morphodynamics

The lower correlations between Q_w and, respectively, Q_s and more notably Q_b at GS2 suggest a direct impact of proglacial morphodynamic processes on downstream transport signals. Cross-correlations of instantaneous sediment flux time series between GS1 and GS2 (Figure 2b) suggest little delay in Q_s; maximum correlations are significant with values of ca. 0.75 and ca. 0.85 at a lag of ca. 0 days for both melt seasons, while the cross-correlations are symmetrical. Q_b show lower maxima values of ca. 0.4 and ca. 0.3 at 0 lag days, but signals are asymmetrical tending toward negative lags, hence a situation where the signal at GS2 peaks usually later then at GS1. The more marked asymmetry for 2020 is due to the decreasing Q_b flux during the melt season (Figure 2a). This means that the Q_b signal recorded in GS1, unlike the Q_s signal, was both dampened (Figure 2a) and delayed (Figure 2b) as it passed through the forefield.

Viewing the Q_s signals in the frequency domain, Figure 2c suggests high power (ca. 10^5 dB) at the shortest time-scales (ca. 10^{-3} days), followed by a significant decrease in magnitude (ca. 10^{-1} dB at 2×10^{-3} days) before a gradual and linear increase up to 10^5 dB at the seasonal scale. The latter has a slope of about 0.23. The evolution of the signals for GS1 and GS2 are similar in both melt seasons, especially in 2021. This suggests limited filtering of the signal for suspended load. For bedload transport, as for suspended transport, both spectra show a decrease to a timescale of ca. 2×10^{-3} days, followed by a weak and unsteady increase until ca. 10^2 dB at 10^{-1} days; the increase is more marked for the GS1 signal than the GS2 one (slopes of ca. 0.6), suggesting a stronger non-linear filtering compared to suspended sediment load for subdaily scales. From timescales of 10^{-1} to 10^0 days, the power continues to increase albeit at a lower rate in both 2020 and 2021, suggesting a cross-over timescale after which the intensity of the non-linear filtering decreases. At GS2 in 2021, power becomes almost constant for bedload transport until time-scales longer than 10^{-1}.

Figure 2c also shows that diurnal transport cycles are maintained along the forefield, as spectra are all characterized by a peak in power at ca. 10^0 days even if, especially for bedload, damped at GS2 (Figure 2a). However, signal cross-correlations (Figure 2b) suggests that it is unlikely that bedload transport peaks at GS2 are related to the same wave of sediment because of proglacial delay. Indeed, the significant removal of scales of variability at GS2 at time-scales longer than those associated with the diurnal variation suggests little transmission of the signal measured at GS1 through the proglacial forefield to GS2.

5. Insight Into the Mechanisms Driving Forefield Morphodynamic Filtering

Given the above, Figure 3 shows the daily timing difference in peak arrivals within GS1 and GS2 for discharge, suspended sediment load and bedload waves. Discharge shows a good correlation in peak times at GS1 and GS2 for both 2020 ($r = 0.91$) and 2021 ($r = 0.97$), even if in 2021 there is a slight tendency for peaks to occur progressively earlier in the day during the melt seasons. The relationship between GS1 and GS2 for sediment transport

10.1029/2023GL106082

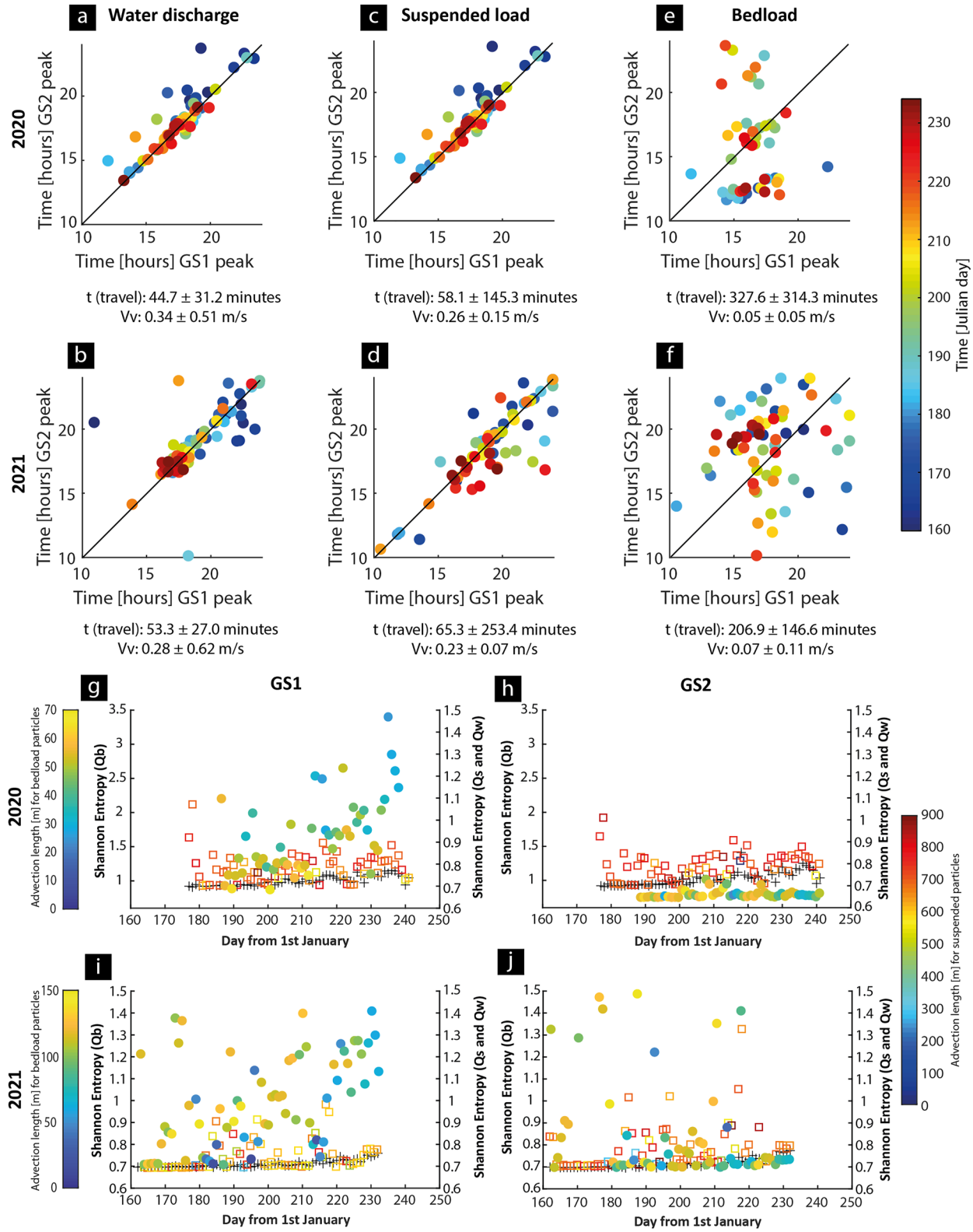

Figure 3. Proglacial filtering mechanisms. Timing difference in peak arrivals between GS1 and GS2 (a–f) and Shannon entropy indexes of signals for melt seasons 2020 and 2021 (g–j; crosses refers to discharge, squares to suspended sediment load and circles to bedload).

is significant for suspended load ($r = 0.93$ in 2020; $r = 0.94$ in 2021), but less significant for bedload ($r = 0.69$ in 2020; $r = 0.53$ in 2021). There are a few days when the daily transport peak at GS2 occurs before the one at GS1 especially for bedload, which is likely to be related to a peak caused by within-reach erosion. In turn, this suggests the presence of multiple source of sediments (Ashmore, 1988, 1991a; Comiti et al., 2019; Mao et al., 2014). Thus, the sediment signals at GS2 contains both the subglacial export signal recorded at GS1, and the signal of erosion and deposition events due to reworking events taking place in the forefield.

If we select only the events in which clear peaks in Q_w, Q_s, and Q_b were identified at GS2 after a peak at GS1, we can calculate the time taken for waves to transit the reach (t(travel), Figure 3). To date, there is no a priori knowledge of virtual velocities in braided stream systems for bedload particles because of their relative long residence time in depositional areas and the difficulty of determining step lengths from field data (Church, 2006; Kasprak et al., 2015; Vázquez-Tarrío et al., 2019). Suspended sediment waves move on average at velocities that are 76.5% and 82.1% of the discharge wave in 2020 and 2021, respectively. Bedload moves at 25% and 14.1% of the discharge wave.

The intense diurnal discharge variation in glacier fed Alpine streams means that if wave velocities are insufficient, sediment exported from the glacier will not reach GS2 before discharge falls below that required for transport, and deposition occurs, delaying the downstream transmission of the bedload export signal (Figure 2b). We can compare the time-scales for bedload transport in Figure 3 with the time-scales of likely sediment transport competence. Daily $Q_w - Q_b$ rating curves established that the critical discharge Q_c required for bedload transport to occur is 3.8 ± 1.25 m^3/s at GS1 and 3.2 ± 1.54 m^3/s at GS2 based on pooling data for 2020 and 2021 (Text S8 in Supporting Information S1). The standard deviations here reflect seasonal changes in characteristics of available sediments and on the degree of armoring of the riverbed (Ashmore, 1988; Hoey & Sutherland, 1991; Vázquez-Tarrío et al., 2019). Figures 3a–3f shows the duration of possible transport ($t \mid t_{Q>Qc}$) for Q_s and Q_b, and the likely advection lengths estimated from wave speeds. For Q_s, advection lengths up to 900 m are generally comparable with the reach length (Figure 1) such that morphodynamic forcing is insufficient to modify the signal of glacial suspended sediment export at GS2 as advection lengths keep up with discharge (Ganti et al., 2014). However, advection lengths are always less than the reach length for Q_b (up to 70 m in 2020 and up to 150 m in 2021) implying morphodynamic forcing of transport, whether due to microscale sediment entrainment-deposition processes or macroscale divergence between flow and sediment transport paths forced by river braiding (e.g., Ashworth, 1996; Bridge & Gabel, 1992). These distances imply transport delays of up to 7–11 days (Figure 2b). This confirms that transport peaks considered in computing virtual velocities (Figure 3) are unlikely to be associated with the same grains because of their longer travel time in the proglacial channel. The preservation of the diurnal evacuation cycles (Figure 2c) is likely related to hydraulically driven transition of former-evacuated bedload waves, progressively moved downstream toward the forefield end by successive discharge waves ("pulses"). This phenomenon also comes with a dampening of the signal (Figures 2a and 2b) suggesting that part of the subglacially exported bedload wave are deposited moving downstream, and highlighted in the field by the sorting of particles going from GS1 to GS2 (Figure 1).

Figures 3g–3j further supports the proglacial filtering of the signal related to subglacial bedload evacuation as the signal entropy (i.e., daily variability) declines due to the forefield. Given the above, the modification of the bedload export signal seems to be driven by particle advection lengths, which in turn depend on grain size and on discharge conditions. It is well established that the intensity of diurnal discharge variation increases during the melt season in glacier-fed streams (Lane & Nienow, 2019; Nienow et al., 1998) because of a progressive reduction in the buffering of glacial melt by snow as the snow-ice interface retreats up glacier and related, a progressive upstream extension of the sub-glacial drainage system (Nienow et al., 1998). Discharge variability constantly increases over time (Figures 3g–3j; Mann-Kendrall tests at $p < 0.05$ confirmed monotonic trends in both 2020 and 2021) suggesting (a) a progressive increase in daily peak discharge, and/or a decrease in daily minimum discharge, and (b) the increasing likelihood of discharge falling below the critical value Q_c later in the season (Figure 2a).

Given this discharge evolution we would expect bedload advection lengths to become progressively longer over time, before dropping toward the end of the season, making transport largely capacity-limited (Perolo et al., 2019). This is exactly the case for GS1, where the transport entropy is higher for bedload than either suspended load or discharge, and it increases systematically through the melt season. In both cases this is combined with a general reduction in advection lengths (Figures 3g and 3i; Mann-Kendrall test $p < 0.05$ for both Shannon entropy and

advection length). However, at GS2, even if there are also seasonally monotonic trends for both entropy and advection lengths (Mann-Kendrall test $p < 0.05$), they are less strong, suggesting less dependence of bedload transport on discharge variation (Figures 3h and 3j). Thus, the seasonal evolution of subglacial bedload export is strongly damped and delayed between GS1 and GS2 (Figures 2b and 2c).

Studies on (pro-)glacial suspended sediment transport involving similar experimental setup shown high variability at daily to seasonal scales (Hodson & Ferguson, 1999; Leggat et al., 2015; Mao & Carillo, 2017). This because the changing upstream conditions, in terms of subglacial discharge (i.e., Hodgkins et al., 2003) and sediment export (i.e., Stott & Mount, 2007) rates, activate the proglacial morphodynamic response buffering, delaying and changing the transport dynamics of subglacially exported particles (e.g., Antoniazza et al., 2019; Ashmore, 1988; Hodson et al., 1998; Misset et al., 2020; Orwin & Smart, 2004). The signal of subglacial suspended sediment export is effectively transmitted downstream, even if some degree of non-linear filtering is detected due to short-lived deposition events at low transport capacity (Guillon et al., 2018; Figures 2a and 2c). In contrast, the short advection lengths for bedload explain why the subglacial bedload export signal at diurnal time-scales is substantially reduced in both melt seasons (Figure 2); it is generally not possible for coarse particles to move fast enough to travel through the proglacial forefield in a single diurnal discharge cycle, a mechanism that is itself conditioned by evolution in seasonal sub-glacial discharge conditions (Figures 3g–5j). However, morphodynamic filtering mechanisms for bedload need to be further investigated.

Given current research in glacial erosion is based upon deployment of monitoring stations located 100s of meters to kilometers downstream of glacier termini (e.g., Herman et al., 2015), it is not clear if they provide reliable erosion rate estimates over relatively short-time scales. The extent to which this is the case will depend on the relative importance of bedload and suspended load export from a glacier, something that remains poorly quantified. In principle, the miscalculation might come from wrongly assuming that subglacial channels always evacuate all eroded sediment (Alley et al., 1997), leading to an overestimation of suspended load as a glacial erosion product. The filtering is likely to be scale limited as in larger glaciers, and notably for ice sheet outlets, the larger spatial melt extent leads to attenuation of diurnal discharge variation (e.g., Cowton et al., 2013) such that subglacial discharge is always greater than the critical value required to maintain transport.

6. Conclusion

The first field-based glacial forefield quantification of continuous suspended load and bedload transport rates provides evidence of an autogenic influence of river morphodynamics on coarse sediment flux, and less on finer sediment flux. The result is a significant dampening and delaying of the signal related to subglacial bedload export, and hence a difference in the erosion rates that would be inferred from sediment transport signals as measurement sizes move donwstream. The modification of coarse sediment flux results from advection lengths that are constrained by both diurnal and seasonal variations in discharge. This is due to (a) proprieties of the subglacial hydrological system which evolve to having baseflows lower and peak flows higher than the critical discharge required for bedload transport, and (b) spatially changing proglacial hydraulic and morphological conditions. These findings are important for the understanding of the sediment connectivity in proglacial margins, especially in terms of natural hazard mitigation and sediment management for hydropower infrastructures, but also for potential geomorphic influences on ecological succession in recently deglaciated terrains. From a glaciological perspective, they suggest that inferences of the relative importance of suspended sediment load and bedload and the timescales of their variation cannot be reliably estimated except where measurements are collected close to glacier termini.

Data Availability Statement

The data used in this study (i.e., water discharge, suspended sediment load and bedload records for 2020 and 2021) are archivied in Zenodo. These are available in (Mancini et al., 2023; Müller & Miesen, 2022).

Acknowledgments
This work was supported by the Foundation Agassiz of the Université de Lausanne and by the Swiss National Science Foundation (SNSF) Grant N°200021_188734 awarded to Stuart N. Lane. The authors are grateful to the authorities of the Commune de Bagnes and of the Canton du Valais for granting access to the field site for the entire duration of data collection. The authors are also obliged to Marc Aguet, Alexandre Armada, Valentin Cina-Colman, Anthony Felix, Mattia Gianini, Valentine Grünwald, Pierre Hauptmann, Isabel Herr, Margaux Hofmann, Frédéric Lardet, Lara Mercier, Boris Ouvry, Gwendoline Perritaz, Alissa Pott, Yaëlle Stampach and Adrijan Selitaj for the help in collecting seismic records and water samples. Rita di Martino and two anonymous reviewers are also thanked for their constructive comments on a previous version of the manuscript.

References

Alley, R. B., Cuffey, K. M., Evenson, E. B., Strasser, J. C., Lawson, D. E., & Larson, G. L. (1997). How glaciers entrain and transport basal sediment: Physical constraints. *Quaternary Science Reviews*, *16*(9), 1017–1038. https://doi.org/10.1016/S0277-3791(97)00034-6

Amundson, J. M., & Iverson, N. R. (2006). Testing a glacial erosion rule using hang heights of hanging valleys, Jasper National Park, Alberta, Canada. *Journal of Geophysical Research*, *111*(F1), F01020. https://doi.org/10.1029/2005JF000359

Antoniazza, G., Bakker, M., & Lane, S. N. (2019). Revisiting the morphological method in two-dimensions to quantify bed-material transport in braided rivers. *Earth Surface Processes and Landforms*, *44*(11), 2251–2267. https://doi.org/10.1002/esp.4633

Ashmore, P. (1991a). Channel morphology and bed load pulses in braided, gravel-bed streams. *Geografiska Annaler—Series A: Physical Geography*, *73*(1), 37–52. https://doi.org/10.2307/521212

Ashmore, P. (1991b). How do gravel-bed rivers braid? *Canadian Journal of Earth Sciences*, *28*(3), 326–341. https://doi.org/10.1139/e91-030

Ashmore, P. E. (1988). Bed load transport in braided gravel-bed stream models. *Earth Surface Processes and Landforms*, *13*(8), 677–695. https://doi.org/10.1002/esp.3290130803

Ashworth, P. J. (1996). Mid-channel bar growth and its relationship to local flow strength and direction. *Earth Surface Processes and Landforms*, *21*(2), 103–123. https://doi.org/10.1002/(SICI)1096-9837(199602)21:2<103::AID-ESP569>3.0.CO;2-O

Beaud, F., Flowers, G., & Venditti, J. G. (2018). Modeling sediment transport in ice-walled subglacial channels and its implication for esker formation and proglacial sediment yields. *Journal of Geophysical Research: Earth Surface*, *123*(12), 3206–3227. https://doi.org/10.1029/2018jf004779

Beaud, F., Fowers, G. E., & Venditti, J. G. (2016). Efficacy of bedrock erosion by subglacial water flow. *Earth Surface Dynamics*, *4*(1), 125–145. https://doi.org/10.5194/esurf-4-125-2016

Beaud, F., Venditti, J. G., Flowers, G. E., & Koppes, M. (2018). Excavation of subglacial bedrock channels by seasonal meltwater flow. *Earth Surface Processes and Landforms*, *43*(9), 1960–1972. https://doi.org/10.1002/esp.4367

Beerbower, J. R. (1964). Cyclothems and cyclic depositional mechanisms in alluvial plain sedimentation. *Kansas Geological Survey Bulletin*, *169*, 31–32.

Bogen, J., Xu, M., & Kennie, P. (2014). The impact of pro-glacial lakes on downstream sediment delivery in Norway. *Earth Surface Processes and Landforms*, *40*(7), 942–952. https://doi.org/10.1002/esp.3669

Bridge, J. S., & Gabel, S. L. (1992). Flow and sediment dynamics in a low sinuosity, braided river: Calamus River, Nebraska Sandhills. *Sedimentology*, *39*(1), 125–142. https://doi.org/10.1111/j.1365-3091.1992.tb01026.x

Carling, P. A., Gupta, N., Atkinson, P. M., & Huang, Q. H. (2016). Criticality in the planform behavior of the Ganges River meanders. *Geology*, *44*(10), 859–862. https://doi.org/10.1130/G38382.1

Carrillo, R., & Mao, L. (2020). Coupling sediment transport dynamics with sediment and discharge sources in a glacial Andean Basin. *Water*, *12*(12), 3452. Article 12. https://doi.org/10.3390/w12123452

Carrivick, J. L., Heckmann, T., Turner, A., & Fischer, M. (2018). An assessment of landform composition and functioning with the first proglacial systems dataset of the central European Alps. *Geomorphology*, *321*, 117–128. https://doi.org/10.1016/j.geomorph.2018.08.030

Church, M. (2006). Bed material transport and the morphology of alluvial river channels. *Annual Review of Earth and Planetary Sciences*, *34*(1), 325–354. https://doi.org/10.1146/annurev.earth.33.092203.122721

Collins, D. N. (2008). Climatic warming, glacier recession and runoff from Alpine basins after the Little Ice Age maximum. *Annals of Glaciology*, *48*, 119–124. https://doi.org/10.3189/172756408784700761

Comiti, F., Mao, L., Penna, D., Dell'Agnese, A., Engel, M., Rathburn, S., & Cavalli, M. (2019). Glacier melt runoff controls bedload transport in Alpine catchments. *Earth and Planetary Science Letters*, *520*, 77–86. https://doi.org/10.1016/j.epsl.2019.05.031

Cook, S. J., Swift, D. A., Kirkbride, M. P., Knight, P. G., & Waller, R. I. (2020). The empirical basis for modelling glacial erosion rates. *Nature Communications*, *11*(1), 759. https://doi.org/10.1038/s41467-020-14583-8

Coulthard, T. J., Lewin, J., & Macklin, M. G. (2005). Modelling differential catchment response to environmental change. *Geomorphology*, *69*(1), 222–241. https://doi.org/10.1016/j.geomorph.2005.01.008

Coulthard, T. J., & Van De Wiel, M. J. (2007). Quantifying fluvial non linearity and finding self-organized criticality? Insights from simulations of river basin evolution. *Geomorphology*, *91*(3–4), 216–235. https://doi.org/10.1016/j.geomorph.2007.04.011

Cowton, T., Nienow, P., Sole, A., Wadham, J., Lis, G., Bartholomew, L., et al. (2013). Evolution of drainage system morphology at a land-terminating Greenlandic outlet glacier. *Journal of Geophysical Research: Earth Surface*, *118*(1), 29–41. https://doi.org/10.1029/2012JF002540

Cudden, J. R., & Hoey, T. B. (2003). The causes of bedload pulses in a gravel channel: The implications of bedload grain-size distributions. *Earth Surface Processes and Landforms*, *28*(13), 1411–1428. https://doi.org/10.1002/esp.521

Delaney, I., Bauder, A., Werder, M. A., & Farinotti, D. (2018). Regional and annual variability in subglacial sediment transport by water for two glaciers in the Swiss Alps. *Frontiers in Earth Science*, *6*(175). https://doi.org/10.3389/feart.2018.00175

Dell'Agnese, A., Mao, L., & Comiti, F. (2014). Calibration of an acoustic pipe sensor through bedload traps in a glacierized basin. *Catena*, *121*, 222–231. https://doi.org/10.1016/j.catena.2014.05.021

Dietze, M. (2018). The R package "eseis"—A software toolbox for environmental seismology. *Earth Surface Dynamics*, *6*(3), 669–686. https://doi.org/10.5194/esurf-6-669-2018

Dietze, M., Lagarde, S., Halfi, E., Laronne, J. B., & Turowski, J. M. (2019). Joint sensing of bedload flux and water depth by seismic data inversion. *Water Resources Research*, *55*(11), 9892–9904. https://doi.org/10.1029/2019WR026072

Ganti, V., Lamb, M. P., & McElroy, B. (2014). Quantitative bounds on morphodynamics and implications for reading the sedimentary record. *Nature Communications*, *5*(1), 3298. Article 1. https://doi.org/10.1038/ncomms4298

Geilhausen, M., Morche, D., Otto, J.-C., & Schrott, L. (2013). Sediment discharge from the proglacial zone of a retreating Alpine glacier. *Zeischrift für Geomorphologie, Supplementary Issue*, *52*(2), 29–53. https://doi.org/10.1127/0372-8854/2012/S-00122

Guillon, H., Mugnier, J.-L., & Buoncristiani, J.-F. (2018). Proglacial sediment dynamics from daily to seasonal scales in a glaciated Alpine catchment (Bossons glacier, Mont Blanc massif, France). *Earth Surface Processes and Landforms*, *43*(7), 1478–1495. https://doi.org/10.1002/esp.4333

Hasbargen, L. E., & Paola, C. (2000). Landscape instability in an experimental drainage basin. *Geology*, *28*(12), 1067–1070. https://doi.org/10.1130/0091-7613(2000)028<1067:LIIAED>2.3.CO;2

Hassan, M. A., Church, M., & Schick, A. P. (1991). Distance of movement of coarse particles in gravel bed streams. *Water Resources Research*, *27*(4), 503–511. https://doi.org/10.1029/90WR02762

Herman, F., Beyssac, O., Brughelli, M., Lane, S. N., Leprince, S., Adatte, T., et al. (2015). Erosion by an Alpine glacier. *Science*, *350*(6257), 193–195. https://doi.org/10.1126/science.aab2386

Hodgkins, R., Cooper, R., Wadham, J., & Tranter, M. (2003). Suspended sediment fluxes in a high-Arctic glacierized catchment: Implications for fluvial sediment storage. *Sedimentary Geology*, *162*(1), 105–117. https://doi.org/10.1016/S0037-0738(03)00218-5

Hodson, A., & Ferguson, R. I. (1999). Fluvial suspended sediment transport from cold and warm-based glaciers in Svalbard. *Earth Surface Processes and Landforms*, *24*(11), 957–974. https://doi.org/10.1002/(SICI)1096-9837(199910)24:11<957::AID-ESP19>3.0.CO;2-J

Hodson, A., Gurnell, A., Tranter, M., Bogen, J., Hagen, J. O., & Clark, M. (1998). Suspended sediment yield and transfer processes in a small High-Arctic glacier basin, Svalbard. *Hydrological Processes*, *12*(1), 73–86. https://doi.org/10.1002/(SICI)1099-1085(199801)12:1<73::AID-HYP564>3.0.CO;2-S

Hoey, T. B., & Sutherland, A. J. (1991). Channel morphology and bedload pulses in braided rivers: A laboratory study. *Earth Surface Processes and Landforms*, *16*(5), 447–462. https://doi.org/10.1002/esp.3290160506

Humphrey, N. F., & Raymond, C. F. (1994). Hydrology, erosion and sediment production in a surging glacier: Variegated Glacier, Alaska, 1982–83. *Journal of Glaciology*, *40*(136), 539–552. https://doi.org/10.3189/S0022143000012429

Hundey, E. J., & Ashmore, P. E. (2009). Length scale of braided river morphology. *Water Resources Research*, *45*(8), W08409. https://doi.org/10.1029/2008WR007521

Jerolmack, D. J., & Paola, C. (2010). Shredding of environmental signals by sediment transport. *Geophysical Research Letters*, *37*(19), L19401. https://doi.org/10.1029/2010GL044638

Kasprak, A., Wheaton, J. M., Ashmore, P. E., Hensleigh, J. W., & Peirce, S. (2015). The relationship between particle travel distance and channel morphology: Results from physical models of braided rivers. *Journal of Geophysical Research: Earth Surface*, *120*(1), 55–74. https://doi.org/10.1002/2014JF003310

Kim, W., Paola, C., Swenson, J. B., & Voller, V. R. (2006). Shoreline response to autogenic processes of sediment storage and release in the fluvial system. *Journal of Geophysical Research*, *111*(F4), F04013. https://doi.org/10.1029/2006JF000470

Lancaster, S. T., & Casebeer, N. E. (2007). Sediment storage and evacuation in headwater valleys at the transition between debris-flow and fluvial processes. *Geology*, *35*(11), 1027–1030. https://doi.org/10.1130/G239365A.1

Lane, S. N., Bakker, M., Gabbud, C., Micheletti, N., & Saugy, J.-N. (2017). Sediment export, transient landscape response and catchment-scale connectivity following rapid climate warming and Alpine glacier recession. *Geomorphology*, *277*, 210–227. https://doi.org/10.1016/j.geomorph.2016.02.015

Lane, S. N., & Nienow, P. W. (2019). Decadal-scale climate forcing of alpine glacial hydrological systems. *Water Resources Research*, *55*(3), 2478–2492. https://doi.org/10.1029/2018WR024206

Lane, S. N., Richards, K. S., & Chandler, J. H. (1996). Discharge and sediment supply controls on erosion and deposition in a dynamic alluvial channel. *Geomorphology*, *15*, 1–15. https://doi.org/10.1016/0169-555X(95)00113-J

Leggat, M. S., Owens, P. N., Stott, T. A., Forrester, B. J., Déry, S. J., & Menounos, B. (2015). Hydro-meteorological drivers and sources of suspended sediment flux in the pro-glacial zone of the retreating Castle Creek Glacier, Cariboo Mountains, British Columbia, Canada. *Earth Surface Processes and Landforms*, *40*(11), 1542–1559. https://doi.org/10.1002/esp.3755

Mancini, D., Dietze, M., Müller, T., Jenkin, M., Miesen, F., Roncoroni, M., et al. (2023). Suspended sediment load and bedload flux records from the Glacier d'Otemma proglacial forefield (summers 2020 and 2021) [Dataset]. Zenodo. https://doi.org/10.5281/zenodo.8380815

Mancini, D., & Lane, S. N. (2020). Changes in sediment connectivity following glacial debuttressing in an Alpine valley system. *Geomorphology*, *352*, 106987. https://doi.org/10.1016/j.geomorph.2019.106987

Mao, L., & Carillo, R. (2017). Temporal dynamics of suspended sediment transport in a glacierized Andean basin. *Geomorphology*, *284*, 116–125. https://doi.org/10.1016/j.geomorph.2016.02.003

Mao, L., Dell'agnese, A., Huincache, C., Penna, D., Engel, M., Niedrist, G., & Comiti, F. (2014). Bedload hysteresis in a glacier-fed mountain river. *Earth Surface Processes and Landforms*, *39*(7), 964–976. https://doi.org/10.1002/esp.3563

Marren, P. M., & Toomath, S. C. (2013). Fluvial adjustments in response to glacier retreat: Skaftafellsjökull, Iceland. *Boreas*, *42*(1), 57–70. https://doi.org/10.1111/j.1502-3885.2012.00275.x

Métivier, F. (1999). Diffusivelike buffering and saturation of large rivers. *Physical Review E*, *60*(5), 5827–5832. https://doi.org/10.1103/PhysRevE.60.5827

Misset, C., Reckinh, A., Legout, C., Bakker, M., Bodereau, N., Borgnier, L., et al. (2020). Combining multi-physical measurements to quantify bedload transport and morphodynamics interactions in an Alpine braiding river reach. *Geomorphology*, *351*, 106877. https://doi.org/10.1016/j.geomorph.2019.106877

Moon, T. (2017). Saying goodbye to glaciers. *Science*, *356*(6338), 580–581. https://doi.org/10.1126/science.aam9625

Müller, T., & Miesen, F. (2022). Stream discharge, stage, electrical conductivity & temperature dataset from Otemma glacier forefield, Switzerland (from July 2019 to October 2021) [Dataset]. Zenodo. https://doi.org/10.5281/zenodo.6202732

Nienow, P. W., Sharp, M., & Willis, I. (1998). Seasonal changes in the morphology of the subglacial drainage system, Haut Glacier d'Arolla, Switzerland. *Earth Surface Processes and Landforms*, *23*(9), 825–843. https://doi.org/10.1002/(SICI)1096-9837(199809)23:9<825::AID-ESP893>3.0.CO;2-2

Orwin, J. F., & Smart, C. C. (2004). Short-term spatial and temporal patterns of suspended sediment transfer in proglacial channels, Small River Glacier, Canada. *Hydrological Processes*, *18*(9), 1521–1542. https://doi.org/10.1002/hyp.1402

Parsons, A. J., Cooper, J., Wainwright, J., & Sekiguchi, T. (2018). Virtual velocity of sand in water. *Earth Surface Processes and Landforms*, *43*(3), 755–761. https://doi.org/10.1002/esp.4262

Perolo, P., Bakker, M., Gabbud, C., Moradi, G., Rennie, C., & Lane, S. N. (2019). Subglacial sediment production and snout marginal ice uplift during the late ablation season of a temperate valley glacier. *Earth Surface Processes and Landforms*, *44*(5), 1117–1136. https://doi.org/10.1002/esp.4562

Phillips, J. D. (2003). Sources of nonlinearity and complexity in geomorphic systems. *Progress in Physical Geography: Earth and Environment*, *27*(1), 1–23. https://doi.org/10.1191/0309133303pp340ra

Richards, K. (1984). Some observations on suspended sediment dynamics in Storbregrova, Jotunheimen. *Earth Surface Processes and Landforms*, *9*(12), 101–112. https://doi.org/10.1002/esp.3290090202

Rickenmann, D. (1991). Hyperconcentrated flow and sediment transport at steep slopes. *Journal of Hydraulic Engineering*, *117*(11), 1419–1439. https://doi.org/10.1061/(ASCE)0733-9429(1991)117:11(1419)

Riihimaki, C. A., MacGregor, K. R., Anderson, R. S., Anderson, S. P., & Loso, M. G. (2005). Sediment evacuation and glacial erosion rates at a small alpine glacier. *Journal of Geophysical Research*, *110*(F3), F03003. https://doi.org/10.1029/2004JF000189

Roussel, E., Marren, P. M., Cossart, E., Toumazet, J.-P., Chenet, M., Grancher, D., & Jomelli, V. (2018). Incision and aggradation in proglacial rivers: Post-Little Ice Age long-profile adjustments of Southern Iceland outwash plains. *Land Degradation & Development*, *29*(10), 3753–3771. https://doi.org/10.1002/ldr.3127

Stott, T., & Mount, N. (2007). Alpine proglacial suspended sediment dynamics in warm and cool ablation seasons: Implications for global warming. *Journal of Hydrology*, *332*(3), 259–270. https://doi.org/10.1016/j.jhydrol.2006.07.001

Straub, K. M., Duller, R. A., Foreman, B. Z., & Hajek, E. A. (2020). Buffered, incomplete and shredded: The challenges of reading an imperfect stratigraphic record. *Journal of Geophysical Research: Earth Surface*, *135*(3), e2019JF005079. https://doi.org/10.1029/2019JF005079

Swift, D. A., Nienow, P. W., & Hoey, T. B. (2005). Basal sediment evacuation by subglacial meltwater: Suspended sediment transport from Haut Glacier d'Arolla, Switzerland. *Earth Surface Processes and Landforms*, *30*(7), 867–883. https://doi.org/10.1002/esp.1197

Van De Wiel, M. J., & Coulthard, T. J. (2010). Self-organized criticality in river basins: Challenging sedimentary records of environmental change. *Geology*, *38*(1), 87–90. https://doi.org/10.1130/G30490.1

Van Dijk, M., Postma, G., & Kleinhans, M. G. (2009). Autocyclic behaviour of fan deltas: An analogue experimental study. *Sedimentology*, *56*(5), 1569–1589. https://doi.org/10.1111/j.1365-3091.2008.01047.x

Vázquez-Tarrío, D., Recking, A., Liébault, F., Tal, M., & Menéndez-Duarte, R. (2019). Particle transport in gravel-bed rivers: Revisiting passive tracer data. *Earth Surface Processes and Landforms*, *44*(1), 112–128. https://doi.org/10.1002/esp.4484

Zemp, M., Haeberli, W., Hoelzle, M., & Paul, F. (2006). Alpine glaciers to disappear within decades? *Geophysical Research Letters*, *33*(13), L13504. https://doi.org/10.1029/2006GL026319

References From the Supporting Information

Aki, K., & Richards, P. G. (2002). *Quantitative seismology*. University Science Book.

Antoniazza, G., Mancini, D., Rieckmann, D., Nicollier, T., Boss, S., Turowski, J. M., et al. (2023). Anatomy of a bedload transport event: An alpine watershed-scale seismic-array monitoring. *Journal of Geophysical Research: Earth Surface*, *128*(8), 22022JF007000. https://doi.org/10.1029/2022JF007000

Bakker, M., Gimbert, F., Geay, T., Misset, C., Zanker, S., & Recking, A. (2020). Field application and validation of a seismic bedload transport model. *Journal of Geophysical Research: Earth Surface*, *125*(5), e2019JF005416. https://doi.org/10.1029/2019JF005416

Beaton, A. E., & Tukey, J. W. (1974). The fitting of power series, meaning polynomials, illustrated on band-spectroscopic data. *Technometrics*, *16*(2), 147–185. https://doi.org/10.2307/1267936

Beven, K., & Binley, A. (1992). The future of distributed models: Model calibration and uncertainty prediction. *Hydrological Processes*, *6*(3), 279–298. https://doi.org/10.1002/hyp.3360060305

Beven, K., & Binley, A. (2014). GLUE: 20 years on. *Hydrological Processes*, *28*(24), 5897–5918. https://doi.org/10.1002/hyp.10082

Burtin, A., Hovius, N., & Turowski, J. M. (2016). Seismic monitoring of torrential and fluvial processes. *Earth Surface Dynamics*, *4*(2), 285–307. https://doi.org/10.5194/esurf-4-285-2016

Clifford, N. J., Richards, K. S., Brown, R. A., & Lane, S. N. (1995). Scales of variation of suspended sediment concentration and turbidity in a glacial meltwater stream. *Geografiska Annaler—Series A: Physical Geography*, *77*(1/2), 45–65. https://doi.org/10.2307/521277

Dietze, M., Gimbert, F., Turowski, J. M., Stark, K. A., Cadol, D., & Laronne, J. B. (2019). The seismic view on sediment laden ephemeral flows—Modelling of ground motion data for fluid and bedload dynamics in the Arroyo de los Pinos. [Computer software manual]. (Paper to SEDHYD conference) Retrieved from http://micha-dietze.de/pages/publications/other/Dietze_et_al_2019b.pdf

Fenn, C. R., Gurnell, A. M., & Beecroft, I. R. (1985). An evaluation of the use of suspended sediment rating curves for the prediction of suspended sediment concentration in a proglacial stream. *Geografiska Annaler—Series A: Physical Geography*, *67*(1/2), 71–82. https://doi.org/10.2307/520467

Ferguson, R. I. (1994). Critical discharge for entrainment of poorly sorted gravel. *Earth Surface Processes and Landforms*, *19*(2), 179–186. https://doi.org/10.1002/esp.3290190208

Gimbert, F., Tsai, V. C., & Lamb, M. P. (2014). A physical model for seismic noise generation by turbulent flow in rivers. *Journal of Geophysical Research: Earth Surface*, *119*(10), 2209–2238. https://doi.org/10.1002/2014JF003201

Gurnell, A. M. (1982). The dynamics of suspended sediment concentration in a proglacial stream system. In J. W. Glen (Ed.), *Hydrological aspects of alpine and high-mountain areas*, *89* (p. 59). Wiley.

Lagarde, S., Dietze, M., Gimbert, F., Laronne, J. B., Turowski, J. M., & Halfi, E. (2021). Grain-size distribution and propagation effects on seismic signals generated by bedload transport. *Water Resources Research*, *57*(4), e2020WR028700. https://doi.org/10.1029/2020WR028700

McKay, M. D. (1992). Latin hypercube sampling as a tool in uncertainty analysis of computer models. In *Proceedings of the 24th conference on winter simulation* (pp. 557–564). https://doi.org/10.1145/167293.167637

Sanchez-Sesma, F. J., Weaver, R. L., Kawase, H., Matsushima, S., Luzon, F., & Campillo, M. (2011). Energy partition among elastic waves for dynamic surface loads in a semi-infinite solid. *Bulletin of the Seismological Society of America*, *101*(4), 1704–1709. https://doi.org/10.1785/0120100196

Schmandt, B., Gaeuman, D., Stewart, R., Hansen, S. M., Tsai, V. C., & Smith, J. (2017). Seismic array constraints on reach-scale bedload transport. *Geology*, *45*(4), 299–302. https://doi.org/10.1130/G38639.1

Stott, T., Nuttall, A.-M., Eden, N., Smith, K., & Maxwell, D. (2008). Suspended sediment dynamics in the morteratsch pro-glacial zone, Bernina Alps, Switzerland. *Geografiska Annaler—Series A: Physical Geography*, *90*(4), 299–313. https://doi.org/10.1111/j.1468-0459.2008.00347.x

Taylor, J. R. (1997). *An introduction to error analysis: The study of uncertainties in physical measurements*. University Science Books.

Treitel, S., & Lines, L. (2001). Past, present, and future of geophysical inversion—A new millennium analysis. *Geophysics*, *66*(1), 21–24. https://doi.org/10.1190/1.1444898

Tsai, V. C., Minchew, B., Lamb, M. P., & Ampuero, J.-P. (2012). A physical model for seismic noise generation from sediment transport in rivers. *Geophysical Research Letters*, *39*(2), L02404. https://doi.org/10.1029/2011GL050255